

# Linear estimation of fatigue for the design and evaluation of controllers in wind turbines

Irene Miquelez-Madariaga<sup>1</sup>, Jesús Arellano<sup>2,1</sup>, Daniel Lacheta-Lecumberri<sup>3,1</sup>, and Jorge Elso<sup>1</sup>

<sup>1</sup>Universidad Pública de Navarra

<sup>2</sup>Siemens Gamesa Renewable Energy

<sup>3</sup>VORS Control

**Correspondence:** Irene Miquelez-Madariaga (irene.miquelez@unavarra.es)

**Abstract.** This work presents a methodology to (i) ~~estimate~~-predict fatigue using linear frequency-domain dynamical models and (ii) generate control specifications directly linked to the mechanical fatigue caused by driving loads for a wind turbine applications. The method is intended for frequency domain controller design techniques such as QFT or  $H_\infty$  and is based on Dirlik's method for fatigue assessment. The main advantage of using the frequency domain approach is that the need of ~~computationally expensive processes such as the generation of~~ for computationally expensive processes such as generating turbulent wind fields or aeroelastic simulations is reduced. As a consequence, the controller design ~~method~~-process becomes more agile. The ~~method~~-technique has been validated by designing controllers for the reference 15MW wind turbine based on fatigue specifications, obtaining simulation results with OpenFAST and comparing the fatigue results from a rainflow algorithm with the linear estimation. Fatigue has been reduced by 22% to 35% at different wind speeds corresponding to ~~above-rated~~-the ~~above-rated~~ operation. The mean fatigue estimation error is 1.07%, proving the method is ~~suitable for a~~-a reliable support tool ~~to guide~~ wind turbine control ~~application~~design.

## 1 Introduction

The design of wind turbines is an inherently multiobjective problem. ~~In order to~~-To reduce the Levelized Cost of Energy (LCoE, Bruck (2018)), wind turbines should be designed to maximize the generated power and to minimize design, production and operation expenses. When the design focuses specifically on the control strategies, these main objectives are translated into maximizing generated power, regulating the generator speed, and reducing the driving mechanical loads.

Even though the design of controllers for wind turbines is a well-known problem in the academic literature and there exist plenty of different proposals (?), frequency domain methods stand out due to some advantageous characteristics (Song (2022); Singh (2016)). The first one is ~~the fact~~ that experimental models of the system are obtained by modal identification or similar techniques (?). Therefore, they are directly represented in the frequency domain and can be used with little post-processing. The second advantage, which might be the most relevant one, is that wind theoretical models are described by means of the power spectrum (Kaimal (1972); Mann (1998)). Then, with the three main elements of the design process -system, controller, and disturbance- defined in the frequency domain, computationally-heavy simulations are not required, making the design process agile and allowing multiple iterations.

25 ~~In this context, designing controllers that ensure a reduction of the mechanical fatigue can be a challenge~~ However, controller design is still somewhat disconnected from the evaluation of its performance. Therefore, even when cycles of redesign can be performed quickly, the designer often has little clue about the changes leading to a better controller. According to the standard (IEC (2020)), fatigue must be assessed ~~by means of using~~ aeroelastic simulation of turbulent wind fields. ~~Both the~~ The generation of the wind fields and their simulation are time-consuming steps ~~that are~~ incompatible with a swift workflow. Besides, ~~in order~~ to get the fatigue indicator, load cycles are quantified using the nonlinear rainflow counting algorithm and the Wöhler curve.

All in all, a gap exists between the controller design environment, which uses linear frequency-domain models, and the evaluation environment, which requires nonlinear time-domain simulations. Some work has been done to solve this problem for a general wind turbine design application (~~Tibaldi (2016)~~). ~~This work proposes a link between the design and the evaluation environments by providing a method~~ Tibaldi (2016); ~~?~~, but it has not targeted the design of control specifications. The main contribution of this article is a method that allows to evaluate fatigue using linear models, which allows to design control specifications for a target fatigue reduction and ~~to establish controller design specifications that are set in the frequency domain and are at the same time related to mechanical fatigue~~. ~~perform a fast evaluation of the obtained controller via a linear estimation of the fatigue.~~ In both cases, the calculation of fatigue is based on the use of frequency domain models. The proposed method has two main characteristics: (1) it ~~allows to identify~~ identifies the range of frequencies in which the specification contributes more to the overall fatigue, and (2) it ~~allows to quantify~~ quantifies the expected fatigue decrease when a change in the specification or the controller is introduced.

In Section 2, a context on fatigue evaluation is presented, focusing on frequency domain methods. Then, in Section 3 the main contributions of this work are described, namely a method for obtaining the sensitivity of the damage equivalent load to changes in the signal spectrum and a way to propose control specifications to reduce fatigue. Section 4 ~~provides a validation of the method based~~ validates the method on the design of controllers for a 15MW wind turbine. Lastly, Section 5 summarizes the main results and conclusions of the work.

## 2 Frequency domain assessment of mechanical fatigue

The IEC 61400 standard for the design of wind turbines (IEC (2020)) states that the mechanical damage caused by fatigue in a specific wind turbine configuration ~~has to~~ must be evaluated by the simulation of turbulent wind fields at different operating points using an aeroelastic model of the wind turbine. ~~The evaluation process established by the standard starts by simulating the operation of the wind turbine in order to obtain~~ Each of the simulations produces a realistic time series of the mechanical loads. Then, the number and amplitude of the load cycles are computed using a rainflow-counting algorithm. Finally, the total accumulated damage is obtained by using the Wöhler curve (Wöhler (1870)) and a PalmgrenMiner linear damage hypothesis (Manson (1994)).

Although this process is compulsory ~~for the certification of~~ to ultimately certify a wind turbine configuration, ~~it might not be the most suitable approach for the current controller s design process, for various reasons~~ the same is not true during

the intermediate step of controller design. Firstly, mechanical damage does not have an explicit relation with most ~~of the~~ design parameters, which means that the effect of a change in the design is unknown until tested in simulation. Additionally, the generation of wind fields and their simulation in the aeroelastic model are time-consuming steps that prevent the design process from being agile, ~~specially~~ especially due to its iterative nature.

The literature on fatigue assessment includes a set of methods that approximate ~~the fatigue with expressions~~ fatigue with expressions that depend on the spectral properties of the load. The most basic approximation is the narrow-band method (Wirsching (1980)), an analytic method that provides ~~a framework for estimating an estimation of~~ the fatigue damage in structures subjected to random stress processes. The method assumes that the stress process is narrow-band, thus simplifying the analysis by treating the stress cycles as approximately sinusoidal with a constant amplitude and frequency. ~~Besides, the narrow-band method draws an analogy to the rainflow counting method used in the time domain. It~~ The method estimates the number of stress cycles and their respective amplitudes using the properties of the narrow-band random processes. ~~Then, the damage caused by fatigue~~  $\Delta D_{NB}$  is

$$\Delta D_{NB} = \nu_0 N_0^{-1} S_0^{-k} (2m_0)^{\frac{k}{2}} \Gamma\left(1 + \frac{k}{2}\right), \quad (1)$$

where  $\nu_0$  is the zero-crossing rate,  $N_0$  is a normalization factor related to the number of cycles,  $S_0$  is the spectral width parameter,  $m_0$  is the zeroth spectral moment,  $\Gamma()$  is the Gamma function and  $k$  is a material exponent of the S-N curve.

Most of the existing methods ~~offer are~~ variations on the narrow-band method ~~to~~, which offer more precise results for wide-band processes (Benasciutti (2005, 2012)). They often follow an empirical approach and are ~~therefore~~ precise when the analyzed load is similar to the training data. Among ~~the empiricals solutions to these empirical solutions for~~ frequency-domain fatigue assessment, Dirlik's work (Dirlik (1985)) is one of the most accurate and widely accepted ~~methods for estimating fatigue damage under random loading conditions~~ ones. It is specifically designed to handle a wide range of frequency ~~contents~~ content. This method provides an efficient and accurate approach to ~~predict~~ predicting fatigue life by leveraging the statistical properties of the stress response. Dirlik uses a probabilistic approach to estimate the distribution of stress cycles, deriving an empirical formula for the probability density function (PDF) of stress ranges in a random loading process. Essentially, it uses the spectral properties of the load and the mechanical properties that define the Wöhler-Curve. The formula accounts for the distribution of peaks and valleys in the stress history, providing a detailed statistical description. The empirical formula for the PDF is given by

$$\Delta D_{Dirlik} = \nu_p N_0^{-1} S_0^{-k} (m_0)^{\frac{k}{2}} \left[ G_1 Q^k \Gamma(1+k) + 2^{\frac{k}{2}} \Gamma\left(1 + \frac{k}{2}\right) (G_2 |R|^k + G_3) \right], \quad (2)$$

where  $G_1$ ,  $G_2$ , and  $G_3$  are empirical ~~constants derived from fitting the model to experimental data~~ expressions depending on the spectral moments derived by Dirlik,  $Q$  is a parameter related to the peak factor, which is derived from the ratio of higher-order spectral moments and characterizes the non-Gaussianity of the stress process and  $R$  is the mean value of the stress process normalized by its standard deviation, describing the relative location of the process mean ~~with respect to~~ concerning the stress amplitude.

### 90 3 Using linear models for the estimation of fatigue and the generation of control specifications

The main input to the frequency-domain fatigue estimation methods presented in Section 2 is the power spectrum of the evaluated load, which can ~~either be estimated or be either obtained~~ from simulation or measured data ~~or inferred from theoretical models~~, or derived from linear models of the plant. Even though the use of simulation data provides closer results to time-domain evaluation, the use of ~~theoretical models narrows the gap between controller design and fatigue estimation~~ linear models is more appropriate in the controller design workflow.

Assuming a linear model of the open loop plant  $G_{y,u}(i\omega)$ , where  $u$  and  $y$  denote the input and output signal respectively, the closed loop transfer function  $T_{y,u}(i\omega)$  is a function of  $G_{y,u}(i\omega)$  and the controller  $C(i\omega)$ . As an example, the effect of wind  $W(i\omega)$  on the generator speed  $\Omega_g(i\omega)$  in the controlled system is

$$T_{\Omega_g, W}(i\omega) = \frac{G_{\Omega_g, W}(i\omega)}{1 + G_{\Omega_g, \beta}(i\omega)C(i\omega)}. \quad (3)$$

100 Similar relations can be obtained for any input-output combination in the system.

If the ~~closed-loop~~ closed-loop transfer function is known, the theoretical auto-spectrum of the output is obtained using the relation

$$S_{yy}(\omega) = |T_{y,u}(i\omega)|^2 S_{uu}(\omega), \quad (4)$$

where  $S_{uu}(\omega)$  is the auto-spectrum of the ~~disturbance~~ input. In the case of wind turbine control, the disturbance ~~the disturbance~~ input is the wind, as well as the waves for offshore wind turbines. Typically, the rotor effective wind speed (or disk average wind speed ~~(?)~~) is used together with linear models. Theoretical models of rotor effective wind speed are obtained from the combination of turbulence models at a single point, such as the Kaimal spectrum, and the spatial coherence models described in the standard. Then, once the output ~~spectrum~~ spectrum is known, fatigue estimation methods such as Dirlik's can be used to assess fatigue.

110 With this information in hand, a new method for ~~the prediction of fatigue~~ fatigue prediction using linear models is proposed. This method has two main goals: (i) detect the frequencies where the load has a greater contribution to fatigue and design according ~~control specifications~~ to control specifications, and (ii) estimate the ~~change in fatigue for a new control configuration so that the number of nonlinear simulations during the design of a satisfactory controller is reduced~~ sensitivity of fatigue to changes in the controller. The method entails the following steps:

115 1. An initial control configuration is assumed, either a baseline controller that needs to be improved or an ~~open-loop plant. The initial controller  $C_0(i\omega)$  (which could be  $C_0(i\omega) = 0$ ) can be simulated to obtain an open-loop plant. An initial simulation is carried out, leading to a set of output time series, from which the~~ initial output spectrum  $S_{yy,0}(\omega)$  ~~Simulation is calculated. Additionally, simulation~~ outputs are used to obtain an initial fatigue evaluation  $D_0$  using the rainflow method.

120 2. The amplitude of the output spectrum at a single frequency  $\omega_0$  is reduced by a 1% by multiplying the value by 0.99, generating a new spectrum  $S_{yy,\omega_0}(i\omega)$ .

3. A new fatigue estimation  $D_{\omega_0}$  is obtained for  $S_{yy,\omega_0}(i\omega)$ .

4. The fatigue sensitivity at a single frequency  $\Delta D_{\%}(\omega)$  is calculated as

$$\Delta D_{\%}(\omega_0) = \frac{D_0 - D_{\omega_0}}{D_0} \cdot 100. \quad (5)$$

125 5. The process is repeated for the whole range of frequencies in which the spectrum is defined, resulting in  $\Delta D_{\%}(\omega)$ , a frequency dependent function that represents the effect of the each frequency component of the spectrum on the total fatigue.

130 Figure 1 shows an example of the proposed method. In the upper plot, a linear model of the system is represented **by means of using** a magnitude Bode plot. The middle plot represents the load power spectrum obtained from simulation data. Lastly, the lower plot contains the fatigue sensitivity obtained as previously described.

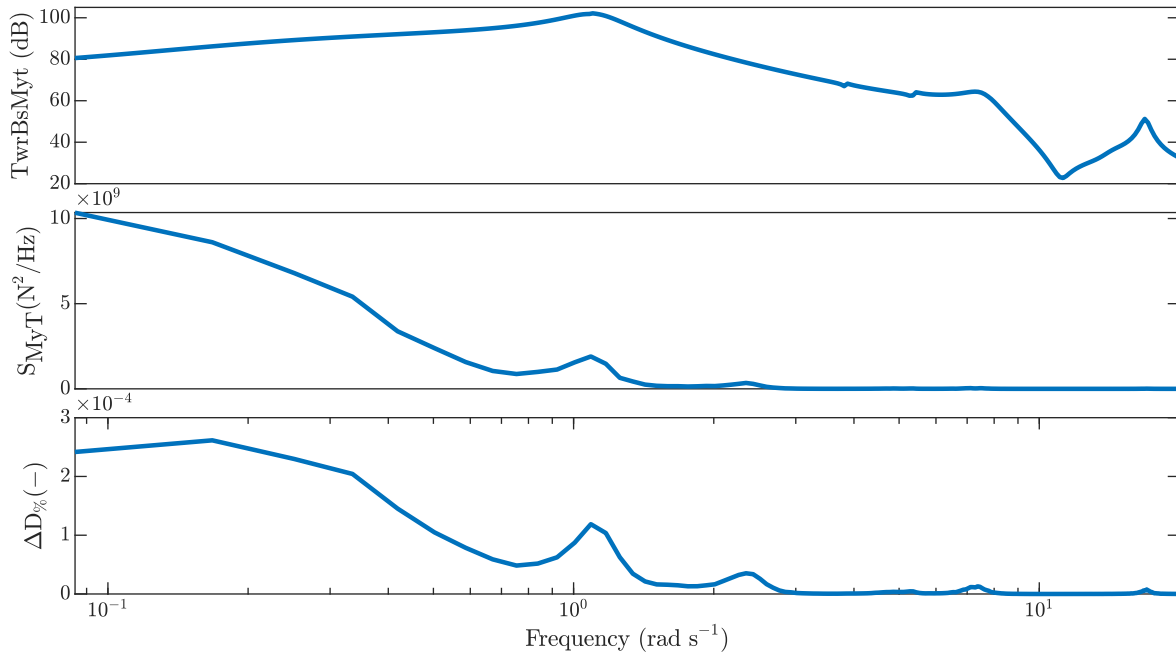


**Figure 1.** This figure shows different aspects of the relation between wind and tower base load. The upper plot shows the magnitude of the closed loop transfer function between wind and load. The middle plot, that represents the load power spectrum, shows how the biggest amplitudes of the load appear at the lower frequencies. The lower plot, ~~which~~ represents how a change **in each frequency of the load would affect to fatigue, shows that higher frequencies lead to higher fatigue** of a 1% in the amplitude of the load at each frequency would modify the total fatigue. Although the shape of  $\Delta D_{\%}$  is similar to the load spectrum, the peaks in the middle to high frequencies have been amplified, as higher frequencies contribute with more cycles than lower frequencies.

Many controller design techniques start by proposing a desired response for the controlled **systemssystem**. This proposal, also known as control specification, can be in the form of parameters of a standard response or, as is the case for QFT

(Quantitative Feedback Theory) or  $H_\infty$ , as an objective frequency response that can be denoted as  $W_y$ . By applying Equation 4, a theoretical output spectrum of the desired response control specification  $S_{W_y}(\omega)$  can be obtained. The achieved attenuation with respect to the baseline controller can be calculated as

$$\Delta S_{W_y}(\omega) = \frac{S_{yy,0}(\omega) - S_{W_y}(\omega)}{S_{yy,0}(\omega)} \cdot 100. \quad (6)$$

Under the assumption of linearity, which The linearity in the relation between fatigue and the amplitude of the spectrum has been tested via simulation, the fatigue by changing the amplification or attenuation factor in the second step of the method.  
 140 In all cases, the increase or decrease of fatigue was proportional to the chosen modification factor. Under the paradigm of linearity, the fatigue variation obtained with the control specification can be calculated as

$$\Delta D_{W_y} = \sum_{\omega} \Delta D_{\%}(\omega) \cdot \Delta S_{W_y}(\omega), \quad (7)$$

and the actual fatigue linear fatigue prediction would be

$$D_{W_y} = \sum_{\omega} \Delta D_{\%}(\omega) \cdot \Delta S_{W_y}(\omega) D_0. \quad (8)$$

145 Using again Equation 4, Equation 7 can be rewritten as

$$\Delta D_{W_y} = \sum_{\omega} \Delta D_{\%}(\omega) \cdot \frac{|T_{yu,i}(i\omega)|^2 - |W_y(i\omega)|^2}{|T_{yu,i}(i\omega)|^2}, \quad (9)$$

where  $\Delta D_{\%}(\omega)$  depends on the initial set of simulations and  $\frac{|T_{yu,i}(i\omega)|^2 - |W_y(i\omega)|^2}{|T_{yu,i}(i\omega)|^2}$  depends exclusively on linear models. With this result, the second objective for the method has been achieved.

#### 4 Validation for the 15MW reference wind turbine

150 The validation of the method proposed in this work is performed by using QFT for the design of linear controllers based on the fatigue specifications. The performance of the controllers is evaluated by their simulation in aeroelastic code (OpenFAST (2024)) and the post-processing post-processing of the resulting time series with a rainflow counting algorithm. For that purpose, the 15MW-15 MW reference wind turbine with the ROSCO controller (Abbas (2022)) is used.

##### 4.1 Sistem description

155 The wind turbine model used for this study is the IEA 15MW reference wind turbine (Gaertner (2020)). This turbine is an offshore, monopile model with three blades and a horizontal axis. The most relevant parameters of the model are gathered in Table 1.

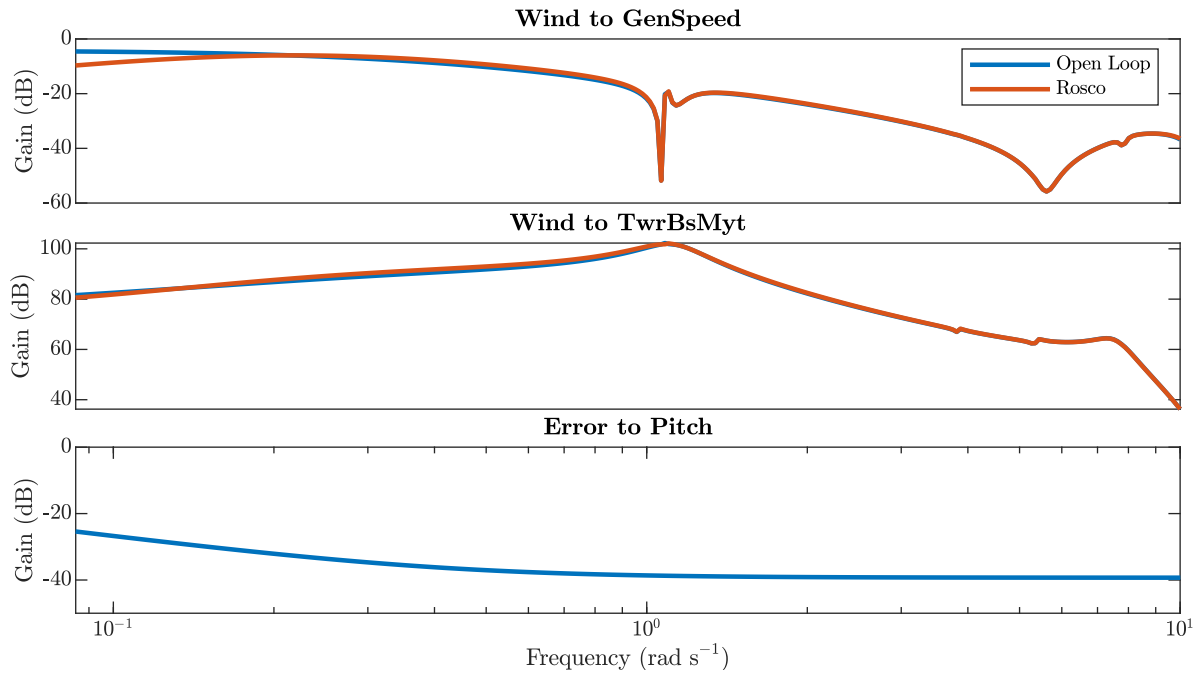
Parameter	Value
Rotor diameter	240 m
Hub height	150 m
Cut-in rotor speed	5 rpm
Rated rotor speed	7.56 rpm

**Table 1.** Value of the main parameters of the 15MW reference wind turbine.

Initially, this wind turbine operates using the reference Open-Source Controller (ROSCO) as a baseline control, which was developed ~~with the aim of offering to offer~~ a modular control structure, with an industry-level performance and compatibility with the OpenFAST design and simulation environment. ROSCO includes the control strategies corresponding to the main operating regions of a wind turbine, from ~~low-speed-low-speed~~ winds (Region 1) to ~~above-rated-above-rated~~ wind speed (Region 3). There are two main control strategies, corresponding to pitch and torque controllers. Torque control is especially relevant at lower wind speeds, in which a ~~quadratic control law is used to ensure~~ maximal power production ~~is sought after~~. ROSCO offers different strategies for below rated operation, among which the quadratic control law has been chosen. Pitch control is used at ~~above-rated-above-rated~~ wind speeds to ensure a constant generator speed and nominal power production. ~~Besides~~Additionally, ROSCO includes switching, filtering and load reduction strategies, such as the Active Tower Damping (ATD), which is typically used to reduce the tower base bending moment at the first fore-aft natural frequency of the tower.

For the purpose of this work, which is linear fatigue assessment, the analysis focuses on ~~above-rated-the above-rated~~ operation. There, the control strategy consists ~~in of~~ a set of linear controllers with scheduled gain to face the nonlinear dynamics of the wind turbine. Typically, these controllers follow a PI structure in which the integrator rejects the effect of wind in the lower frequencies and the zero increases the phase margin of the system. Figure 2 shows the magnitude plot of the PI controller ~~(lower plot)~~ operating at a ~~19m19 m/s~~ wind speed ~~(lower plot)~~ and its effect on the generator speed and tower base load. The main effect of the controller can be appreciated in the generator speed plot. There, the red line ~~corresponding to~~corresponding to the ROSCO controller shows the attenuation of the effect of wind on the generator speed at the lower frequencies. To ensure that the new controller design has a big impact on the tower base fatigue and, thus, the method proposed in Section 3 is tested in a challenging scenario, ATD has been deactivated in the baseline controller. As a consequence, a big reduction in fatigue is expected.

The open-loop linear models of the wind turbine have been obtained with the aid of OpenFASTs linearization tool and the closed-loop models have been calculated following the structure represented in Figure 3.



180

**Figure 2.** Effect of the ROSCO controller on the dynamics of the system. The upper plot shows the effect of the PI controller on the generator speed, which is more relevant at the lower frequencies. The middle plot shows the effect of the controller on the tower base bending moment. Lastly, the lower plot shows the magnitude of the feedback controller.

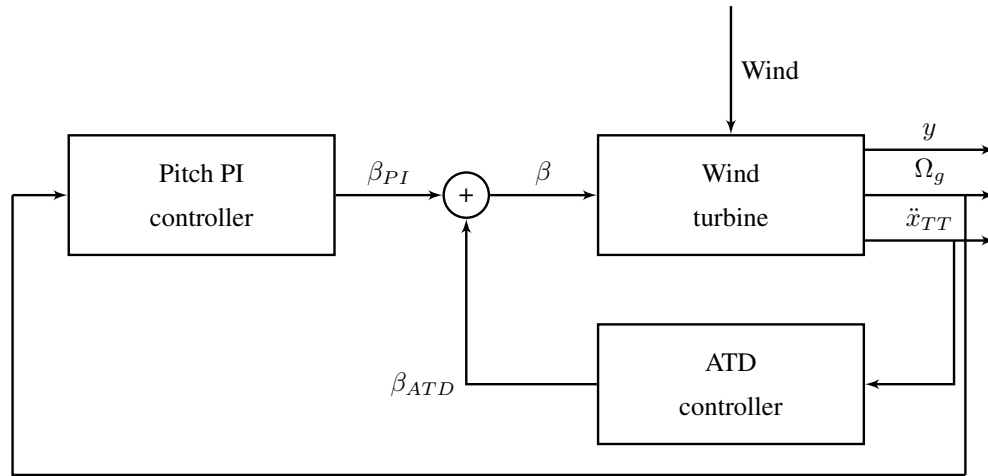


**Figure 3.** Block diagram of the control structure.

## 4.2 QFT fundamentals

Quantitative ~~feedback theory~~ Feedback Theory is a controller design methodology that allows to obtain robust, multivariable ~~and multiobjective solution~~, and multiobjective solutions (Elsø (2017)). The main steps in the design process are:

- 185 1. Obtaining the model of the plant. QFT is based on the use of linear, frequency domain models of the system. Robustness is achieved by using uncertain models during the design.
2. Selecting the design frequencies. QFT design is performed on a discrete set of frequencies as a reference. These frequencies should cover all the relevant dynamics of the system.
- 190 3. Choosing the specifications. In the context of QFT design for ~~win-wind~~ turbine controllers, control specifications are typically upper bounds on the closed-loop disturbance rejection function of the different control objectives. These upper bounds can be constant values or transfer functions and should ideally be linked to performance indicators such as the generator speed standard deviation or the mechanical fatigue of driving components. Besides, a stability specification is imposed as an upper bound on the complementary sensitivity function.
- 195 4. Generation of bounds. At each design frequency, the regions of all controllers meeting each specification ~~is-are~~ found in the complex plane. The boundary of these regions, multiplied by the nominal plant, in the complex plane is called ~~bound and there exists one.~~ One bound is obtained per specification and design frequency.
5. Controller synthesis, also known as loopshaping, consists of tuning the controller parameters until the open-loop transfer function that lies within the bounds at every design frequency.
- 200 6. Checking the specifications. The first validation step uses the uncertain linear model of the plant to ensure that specifications are met at every frequency and not only the design ones.
7. Simulation. If the linear uncertain model of the plant has been derived from a more complex mode (i.e. a nonlinear one), as is the case for wind turbines, a second evaluation of the performance of the controllers is performed via simulation.

The whole process is carried out with the aid of the QFT Toolbox (Yaniv (1997)), which includes graphical tools for the design of specifications and the ~~loopshaping~~loop-shaping process. QFT is inherently an iterative method, more so when several  
205 controllers are being tuned at the same time, and requires some ~~skills in the loopshaping stage~~ practice in the loop-shaping stage before a successful design has been obtained. As a counterpart, it is a versatile and transparent methodology, that grants engineers ~~a~~ full control of the design process.

### 4.3 Controller design

The design of controllers starts with the design of the control specifications ~~, which follows~~ based on the procedure presented  
210 in Section ~~4.3~~. The first step consists ~~on~~ of obtaining a set of simulations of the system with the baseline control. In particular, four wind seeds with length ~~600s~~ 600 s have been simulated at each operating point. Then, these simulations are used to calculate the output spectra and an initial fatigue evaluation. Lastly, the ~~variation of fatigue caused by a change~~ sensitivity of fatigue to changes in the tower base load spectrum  $\Delta D_{\omega}$  is calculated based on the simulation results. Figure 1 shows the relation between the magnitude Bode plot, the ~~spectrum of the load~~ load spectrum and the variation of fatigue for the  
215 simulations corresponding to a 19m/s mean wind speed. While the Bode plot only holds information on the ~~response of the~~

system-system response, the spectrum of the load includes information on the disturbance, ~~showing a higher amplitude in the lower frequencies~~. Besides, as the spectrum has been obtained from simulation data, a peak can be observed at around 2.3 rad/s, ~~that which~~ corresponds to the 3P frequency. Lastly, the lower plot shows how the lower frequencies have ~~the a~~ greater impact on fatigue, but the peaks corresponding to the first fore-aft mode of the tower and the 3P frequency are also relatively relevant.

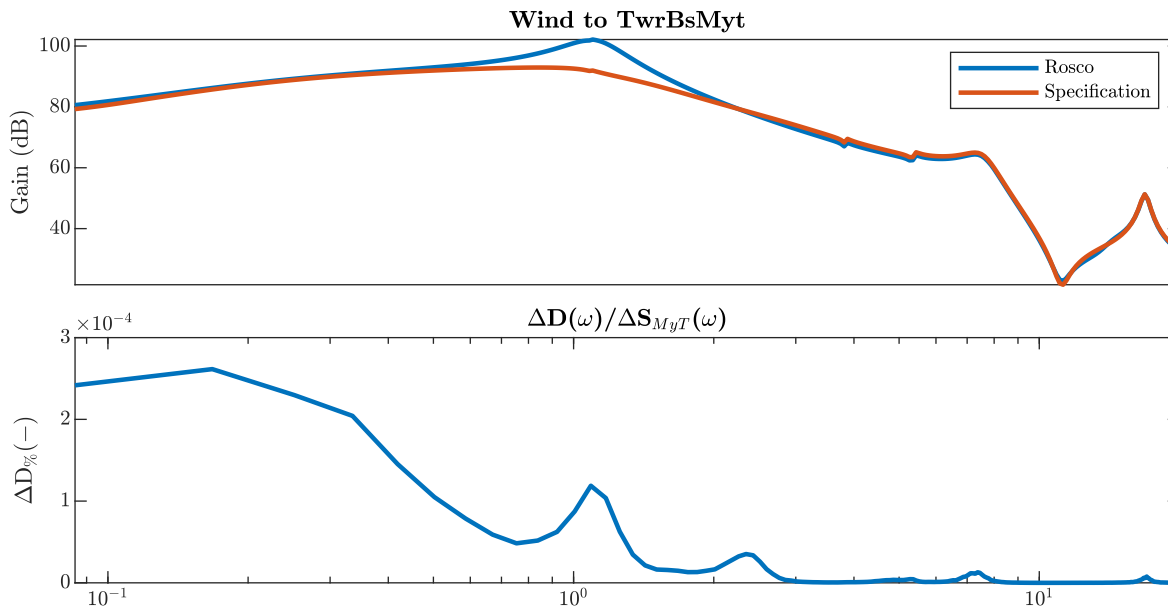
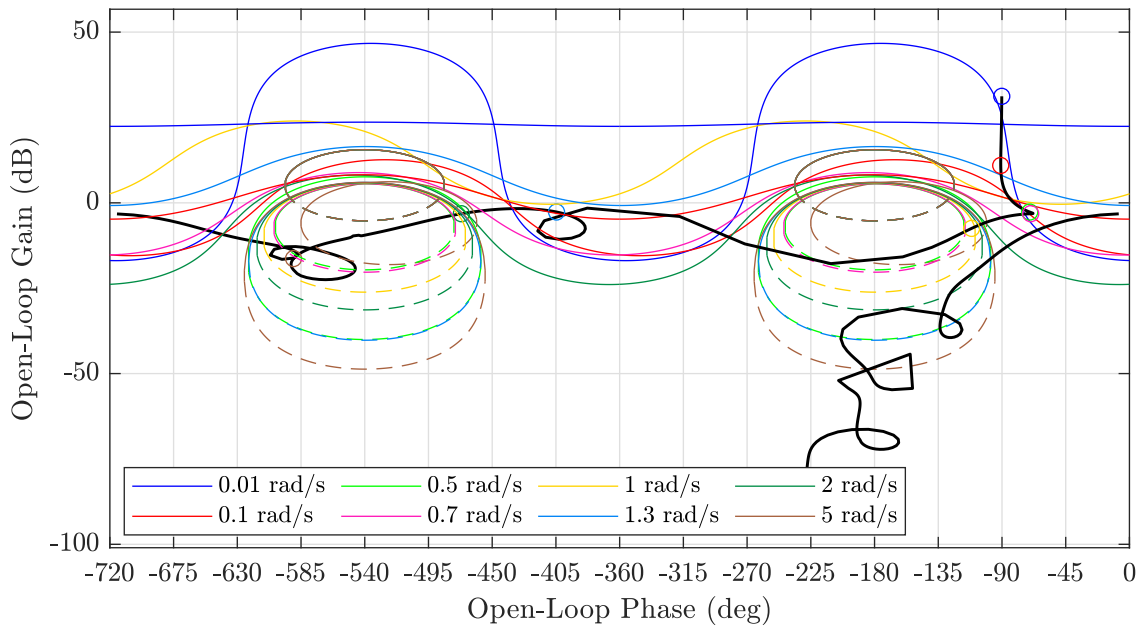


**Figure 4.** Design of the control specification for an operating point corresponding to a 19 m/s wind speed. The control specification has a similar magnitude as the ROSCO controller at all frequencies but the one surrounding the first fore aft mode of the tower (1.1 rad/s).

The design of the control specification  $W_y$ , which takes as a starting point the closed loop transfer function produced by the baseline controller, is based on the information provided by function  $\Delta D\%(\omega)$ . Even though the lower frequencies have the greatest impact on ~~the~~ fatigue (see the lower plot in Figure 4), the designer must keep in mind that the main control objective is to have a constant power production, for which the lower frequencies are key. As a consequence, the control effort is located around the first fore-aft mode of the tower, which appears at approximately 1.1 rad/s. The control specification has been obtained with the aid of the *lpshape* function of the *QFT Toolbox* targeting a fatigue reduction of 15%. A set of notch filters ~~have has~~ been used to reduce the magnitude of the specifications at the chosen frequencies until the desired reduction of fatigue has been obtained ~~or improved~~. The linear fatigue estimation for the specifications at different operating points appears in Table 2.

As already mentioned, power production and, in turn, generator speed regulation are the most relevant objectives in the design of the pitch controllers. As a consequence, they must also be included in the design specifications. In this case, the closed loop transfer function (wind to generator speed) obtained with the ROSCO controller is used as a specification. This way, a ~~better performance than~~ performance similar to the baseline controller is expected in terms of generator speed regulation.



235

**Figure 5.** Bounds for the loopshaping of the main feedback pitch controller. Then main characteristic of this controller is the presence of an integrator to eliminate steady-state error and the use of low frequency poles to increase magnitude and phase below 1 rad/s. The open-loop nominal transfer function meets all bound at all frequencies.

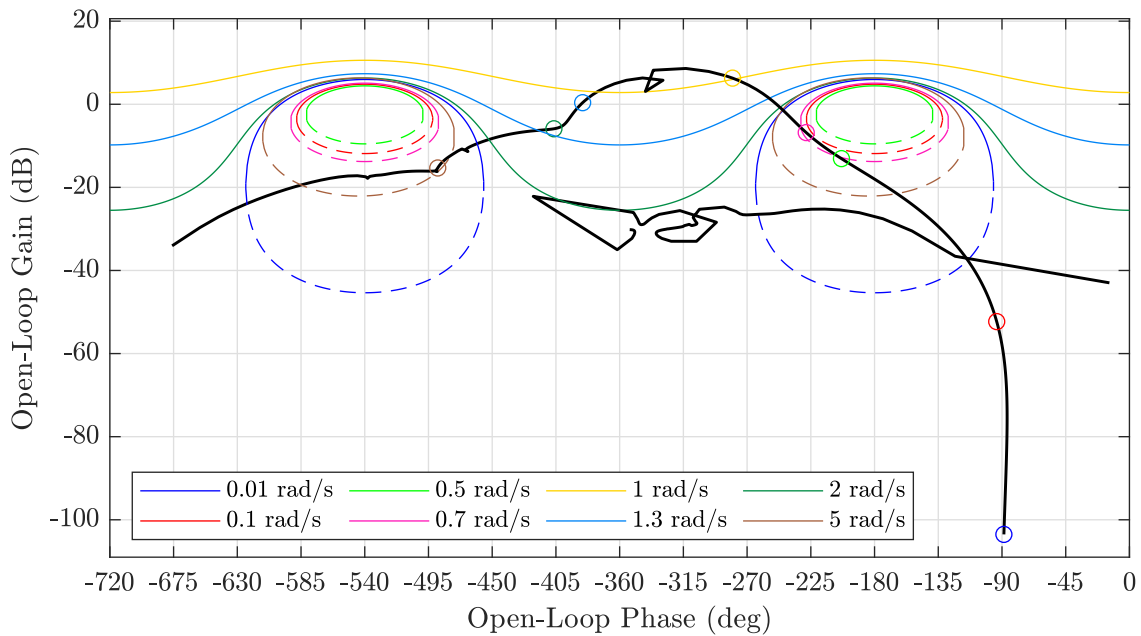


**Figure 6.** Bounds for the loopshaping of the ATD controller. This controller has a pole 0.3276 rad/s and a zero at 4.357 rad/s. The main control effort of the ATD strategy appears close to 1rad/s, at the first fore-aft mode of the tower.

Once the ~~design control~~ specifications for the two control objectives have been ~~obtained~~designed, the bounds for the controllers have been obtained using the procedure described in Section 5.24.2. The bounds are obtained using function *genbounds* and the design of controllers is performed with the aid of *lpshape*. *lpshape* is a graphical design tool that represents the bounds and the open-loop nominal transfer functions in the Nichols plot (gain in dB against phase in degrees). The bounds are the limits between the allowed and forbidden values for the open-loop nominal transfer function. They can have different colours, depending on their corresponding frequency, and solid and dashed lines indicating lower and upper limits. The open-loop nominal transfer function is represented by the solid black line and a set of circular markers at the design frequencies, with the same colour as their corresponding bounds. The design is performed by modifying the position of the markers by adding zeros and poles to the controller.

As two different controllers have been designed for each operating point -the feedback pitch controller and the ATD- the design process is iterative. Due to the lack of ATD controller in the baseline configuration, the design process begins with the tuning of a preliminary ATD controller. Then, several iterations are performed until specifications are met.

Figures 5 and 6 show the final design of the pitch and ATD controllers for the operating point corresponding to a 19 m/s average wind speed. At this wind speed, the pitch controller is

$$C_{\beta}(s) = \frac{-4.8167(s + 0.6)(s^2 + 0.7337s + 0.2441)}{s(s^2 + 1.872s + 2.306)(s^2 + 2.297s + 26.67)}. \quad (10)$$

The ATD controller at the same operating point is

$$C_{ATD}(s) = \frac{0.014187(s + 4.357)}{s + 0.3276}. \quad (11)$$

The ~~bound bounds~~ are met tightly at frequencies ~~surrounding~~surrounding 1 rad/s and with a greater margin for lower frequencies, as seen in Figures 5 and 6. A similar conclusion can be inferred from the Bode plots presented in Figure 7. There, the ~~stars markers~~ represent the design frequencies, which are used for the calculation of bounds and the ~~loop-shaping~~loop-shaping process. As already anticipated, at frequencies below ~~1rad~~1 rad/s, ~~either one or both specifications are at least one of the specifications is~~ met with some margin. At higher frequencies, the tower base load ~~equals exactly is exactly equal to~~ the specification. With a simple enough control structure, a good result is expected in between design frequencies. Figure 7 shows that the QFT controller provides a poorer response than the specification between 0.8 and 1 rad/s and ~~between~~2 and 5 rad/s for the tower base load. However, the ~~overall overall~~ response is better than the specification and shows a significant improvement ~~with respect to concerning the~~ ROSCO controller.

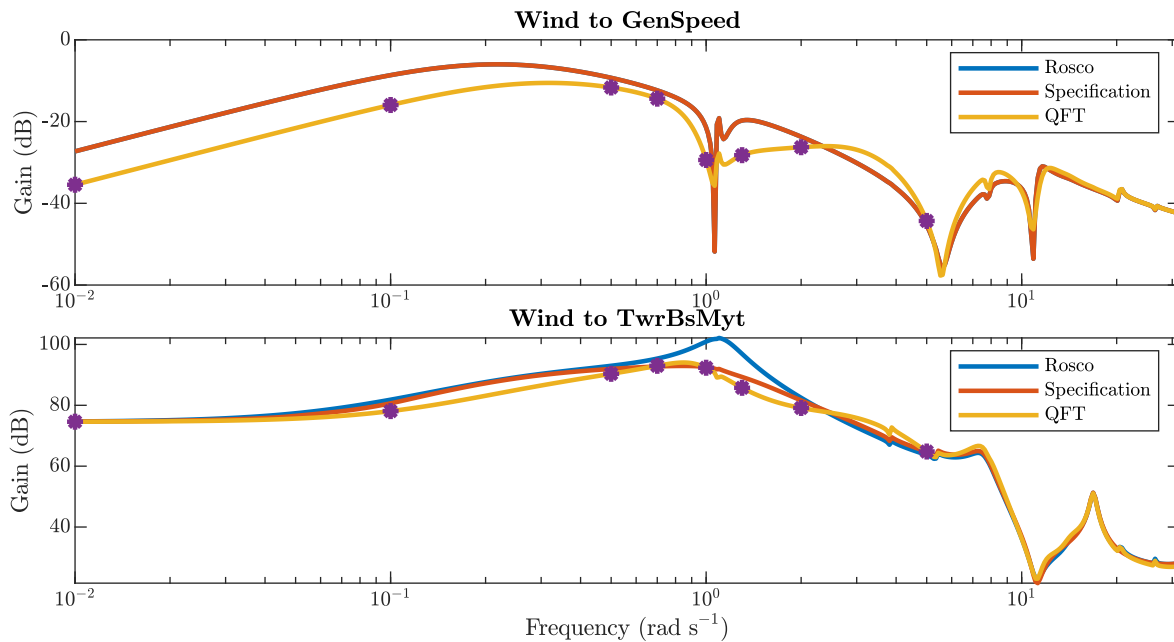


**Figure 7.** Magnitude Bode plot for ROSCO (blue), the design specifications (red) and the QFT controller (yellow) for the generator speed (upper plot) and the tower base load (lower plot). The purple dots show the design frequencies in which the specifications are always met. A simple control structure guarantees that the response between design frequencies is smooth and that specifications are met most of the times.

#### 4.4 Result analysis

265 Once a pitch controller and an ATD controller have been designed for each operating point in the above-rated above-rated region (11 to 25 m/s), they have been integrated in into the aeroelastic simulator using its Simulink interface. Due to the difference structure different structures of the controllers at different operating points, an output blending strategy has been used for the interpolation between controllers. A filtered pitch signal has been used as an interpolation variable.

270 At each operating point, four different seeds have been used for the generation of turbulent wind fields of length 600s and to ensure a reasonable trade-off between results variability due to turbulence and computation time. Each wind file has a 600 s length and a class B turbulent intensity according to the Normal Turbulence Model (NTM, ?) and the IEC:61400:1-2019 standard. Wind fields have been generated using the tool Turbsim (Jonkman (2006)).

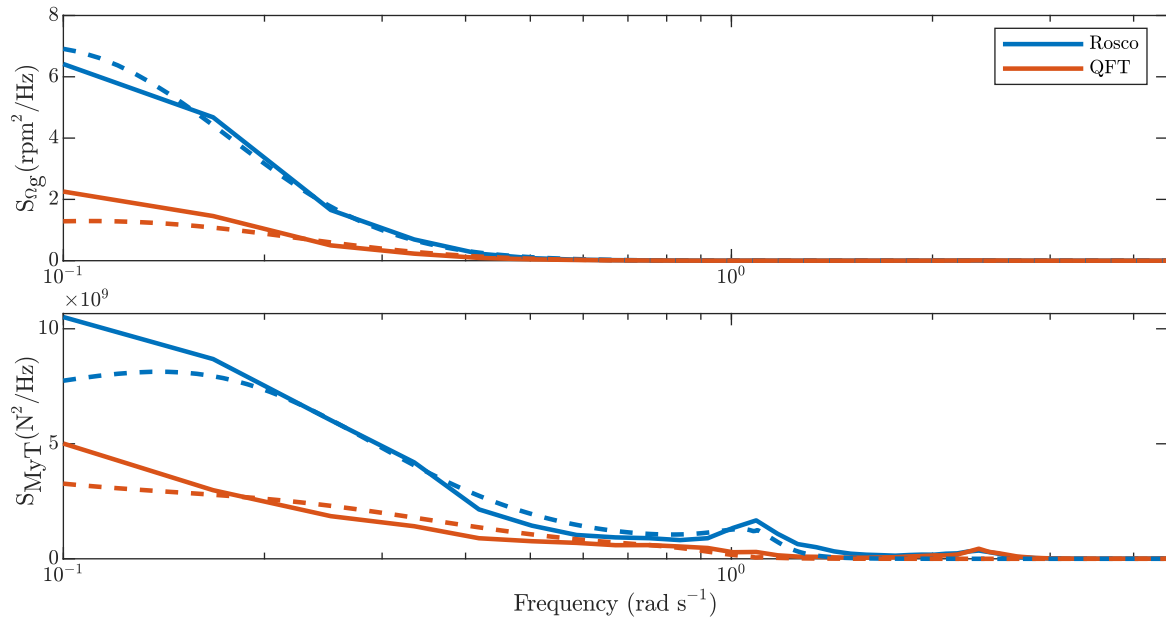


**Figure 8.** Validation of the correspondence between linear (dashed) and nonlinear (solid) models with the ROSCO (blue) and QFT (red) controllers. Besides a good matching between both models, the effect of the QFT controllers can be observed in the lower magnitude of the spectra, especially in frequencies below 0.5 rad/s and in the peak corresponding to the first fore-aft mode of the tower (close to 1 rad/s).

The first step in the analysis of the results consists ~~on~~ of the validation of the relation between the linear and the nonlinear  
 275 models. Figure 8 shows a comparison between the theoretical and simulation spectra of the generator speed and tower base  
 bending moment with the baseline and the QFT controllers at an operating point of 19 m/s. The theoretical spectra have been  
 obtained using the linear model of the wind turbine and the theoretical spectrum of rotor effective wind speed. The simulation  
 spectra have been obtained by ~~applying~~ applying the Welch method to the time series obtained from OpenFAST. Two main  
 conclusions can be extracted from this figure: (i) the QFT controller outperforms ~~the~~ ROSCO controller for both outputs and  
 280 (ii) there exists a good correspondence between the estimation obtained from the linear model and the results of the nonlinear  
 simulation. This second fact is critical for the performance of the proposed fatigue estimation method.

Performance parameters	Operating point (m/s)						Mean
	15	17	19	21	23	25	
Generator speed std	31.54%	-1.91%	-39.48%	-48.96%	-50.07%	-52.18%	
Mean power	0.47%	0.37%	0.05%	-0.17%	-0.42%	-0.46%	
Tower base DEL	-25.91%	-22.24%	-27.75%	-27.28%	-34.71%	-28.84%	
Pitch activity	-8.22%	-0.53%	1.13%	6.66%	1.87%	5.43%	

**Table 2.** Comparison of the main performance indicators for the ROSCO and QFT controllers.

Even though improving the performance of ROSCO is not the main objective of this work, the performance of the QFT controller has been studied to understand the ~~possibilities~~ possibilities of this design technique and ~~the fatigue-based~~ fatigue-based identification. The performance of the controllers has been ~~measured with~~ evaluated using four main indicators. The standard deviation of the generator speed is used as a measure of the quality of the generator speed regulation. Table 2 shows how the standard deviation is reduced for all operating points but 15 m/s, which is closer to the transition between regions. The mean generated power shows small variations at different operating points that cancel each other when calculating the total average. As expected from the linear ~~model~~ fatigue prediction, the fatigue at the tower base is reduced significantly at all operating points, partly due to the absence of ATD in the baseline controller. Lastly, pitch activity is evaluated using the standard deviation of the collective pitch signal, which is significantly reduced at 15 m/s and then increases for wind speeds 19 to 25 m/s. A more thorough analysis of the cost of pitch control should be based on the actuator fatigue, where less favourable results would be expected. Mean values have been obtained assuming a Weibull distribution in mean wind with shape factor of 2.2 and a scale factor of 11.29.

Similar information can be perceived in Figure 9, which represents the simulation outputs for a single wind seed with ~~mean~~ speed a mean speed of 19 m/s. Both the generator speed and the tower base load show smaller deviations from their mean value for the QFT controller, which ~~account for a smaller~~ accounts for a smaller standard deviation and fatigue respectively. ~~Power~~ The power mean value is close to ~~15MW~~ 15 MW in both cases. The presence of the ATD controller in the QFT configuration can be observed in the ripple that appears in the pitch signal, accounting for an increased pitch standard deviation.

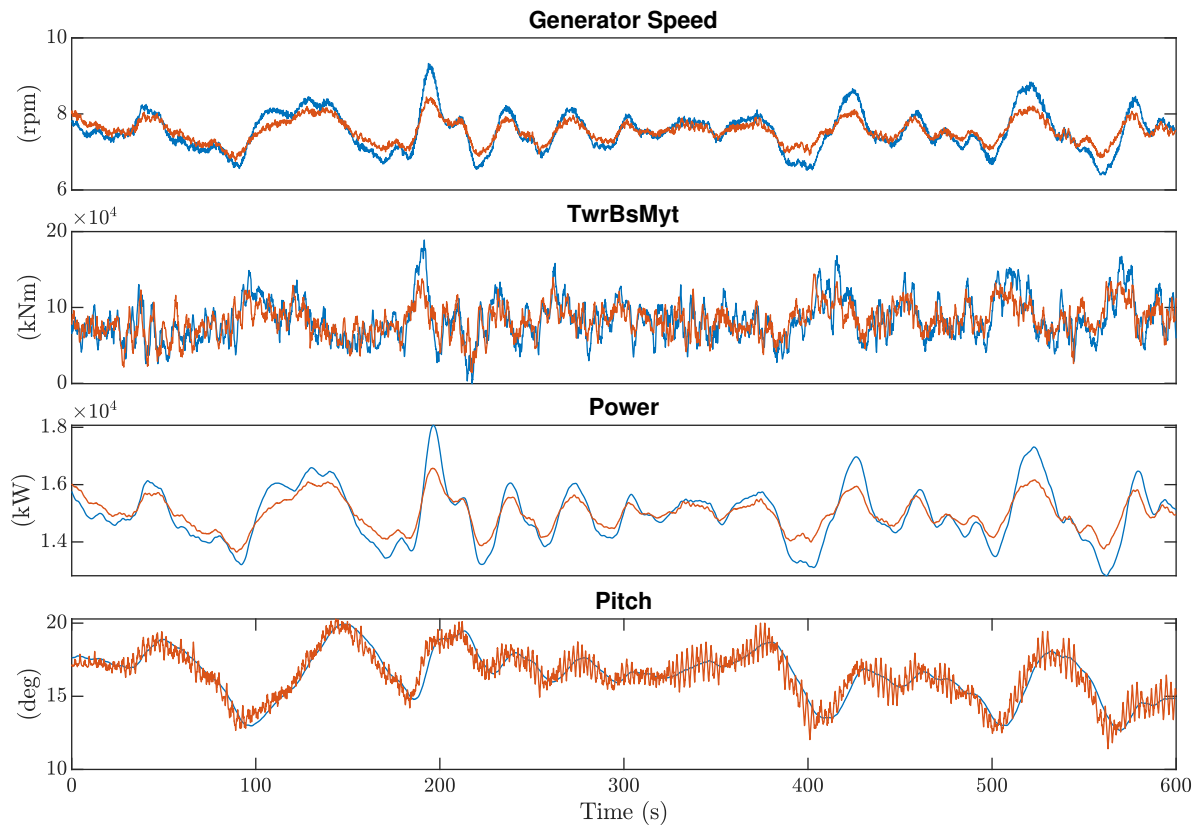


**Figure 9.** Time series of relevant variables in an OpenFAST simulation with mean wind speed 19 m/s. The standard deviation of generator speed and power is visibly smaller for the QFT controller (red) than for ROSCO (blue). Besides, the fatigue in the tower base load should also be reduced as the ATD controller mitigates the bigger peaks in the blue line, that do not appear for the QFT controller. Lastly, the lower plot shows that the use of an ATD controller results on an increased high frequency pitch activity.

300 The main result of this work is the linear prediction of fatigue with the use of linear using linear frequency-domain models.  
 Table 4.4-3 shows the fatigue reduction promised by the specifications, the fatigue reduction estimation provided by the linear approximation-linear estimation of the fatigue reduction for the new controllers and the actual fatigue reduction calculated  
 using a rainflow counting algorithm and the S-N curve. Two main conclusions can be extracted from the data: (i) the fatigue  
 predicted by the linear model is always smaller than the promised by the specifications except from the 15 m/s operating  
 305 point and (ii) the deviation between the linear prediction and the rainflow-based fatigue evaluation is smaller than 2% for all  
 operating points, having an average-average value of 1.07%.

Fatigue estimation	Operating point (m/s)						
	15	17	19	21	23	25	Mean
Specifications	37.37%	10.10%	11.78%	20.55%	35.97%	30.35%	
Linear prediction	24.81%	24.15%	28.60%	27.93%	35.12%	30.36%	
Rainflow evaluation	25.91%	22.24%	27.75%	27.28%	34.71%	28.84%	
Estimation deviation	1.1%	1.91%	0.85%	0.65%	0.41%	1.52%	1.07%

**Table 3.** Fatigue reduction at different operating points. The Table includes information on the fatigue reduction promised by the specification, the reduction estimated with the help of linear models and the actual fatigue reduction as evaluated with a rainflow counting algorithm.

Figure 10 shows a graphical representation of the accuracy of the linear approximation of fatigue by plotting the frequency-domain estimation against the time-domain evaluation. The black line ( $y = x$ ) serves as a reference of a perfect prediction, while the actual data is represented as a star per operating point. Apart from the point corresponding to 15m/s, the linear approximation tends to overestimate the fatigue reduction, although the error remains admissible for controller design purposes.

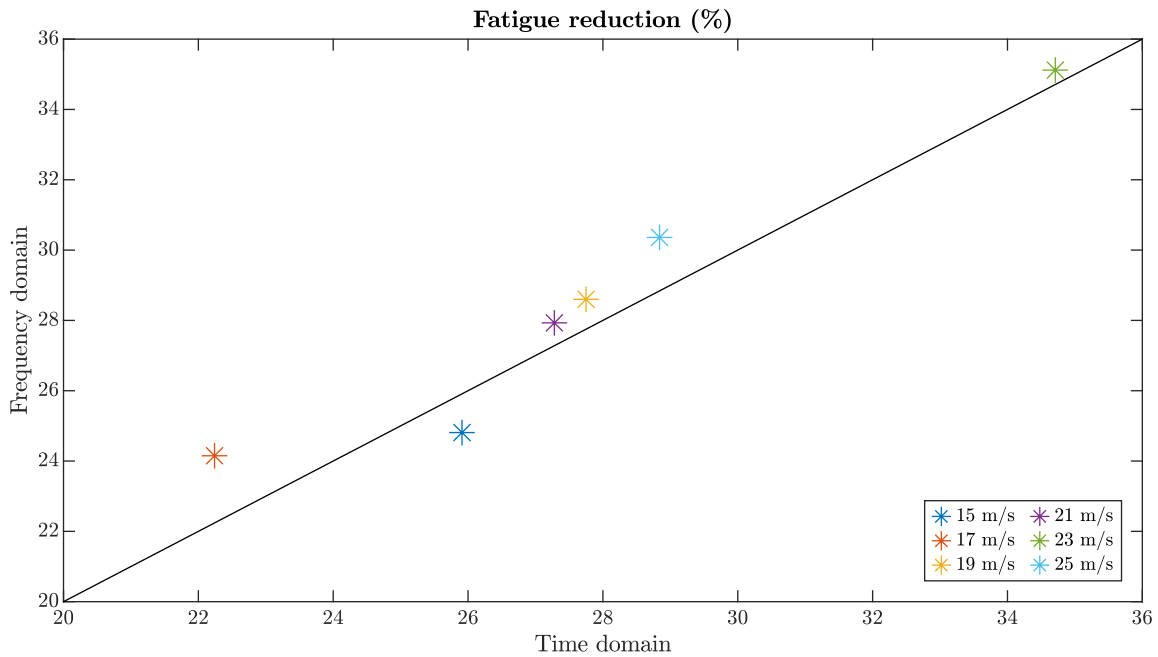


**Figure 10.** Graphical comparison of the linear fatigue estimation (frequency domain linear prediction) and the rainflow-based fatigue assessment (time domain). The black line presents the perfect-estimation reference, while the stars represent the actual relation between the frequency domain and the time domain results for different operating points (Rainflow evaluation).

## 5 Conclusions

This work has presented a method for the estimation of mechanical fatigue based on the use of the linear model of a wind turbine and its controllers and a numerical calculation of the variation of the ~~damaged~~damage with the load spectrum. Then, this method has been used for the design of control specifications.

The method has been validated with the design of pitch controllers for the ~~15MW~~15 MW reference wind turbine. More specifically, the feedback pitch controller and the active tower damping have been designed to improve the performance of the ROSCO PI controller. With the aid of the linear fatigue estimation and the design of specifications, fatigue has been reduced by 22 to 36% at operating points ranging from 15 to 25 m/s mean wind speed. Due to the good correspondence between the linear fatigue prediction and the fatigue evaluation obtained with a rainflow algorithm (under a 2%), a single iteration in the non-linear simulation step has been required. Consequently, the design process has been accelerated significantly, by reducing the number of required simulations to two sets.

The error present in the fatigue estimation can be attributed to ~~two~~three different factors. The first one is that the results provided by the linear model do not exactly match the ones provided by the nonlinear simulator. ~~Besides~~In addition to the numerous non-linearities present in the realistic model of the wind turbine and the complete control structure, other phenomena such as the 3P frequency and the spatial variation of the wind cannot be taken into account by a linear approximation. The second factor is the difference between time-domain and frequency-domain fatigue evaluation methods. The rainflow-counting algorithm has proven to be the best approximation for fatigue estimation and is the reference in the standard. On the other side, due to the fundamental empirical nature of frequency-domain methods, their performance varies significantly depending on the characteristics of the load and the system. While Dirlik's method has proven to provide a good result, the search for a more accurate method remains open. Lastly, the proposed method is based on a linear approximation to fatigue estimation, which can introduce an error.

All in all, the use of linear models for fatigue estimation has proven to be useful and their use can be extended. On the one hand, the use of this frequency domain estimation of fatigue could be included in the iterative design of other wind turbine components, such as structural elements. On the other hand, their use could also be studied for different controller design ~~methologies~~methodologies, the most obvious one being  $H_\infty$ . Lastly, the full potential of the methodology could be achieved for multi-objective design, in which the role of the control system in the fatigue of different elements could be linked to the ~~bussines~~business case of the wind turbine.

*Author contributions.* Irene Miquelez-Madariaga: Conception, simulation data collection, writing. Jesús Arellano: Conception, writing. Daniel Lacheta-Lecumberri: Simulation data collection, proofreading. Jorge Elso: Conception, proofreading.

*Competing interests.* The contact author has declared that none of the authors has any competing interests.

## References

- Bruck, M., Sandborn, P., and Goudarzi, N. (2018). A Levelized Cost of Energy (LCOE) model for wind farms that include Power Purchase Agreements (PPAs). *Renewable Energy*, 122, 131-139.
- 345 Kaimal, J. C., Wyngaard, J. C. J., Izumi, Y., & Coté, O. R. (1972). Spectral characteristics of surfacelayer turbulence. *Quarterly Journal of the Royal Meteorological Society*, 98(417), 563-589.
- Mann, J. (1998). Wind field simulation. *Probabilistic engineering mechanics*, 13(4), 269-282.
- Song, Y., Jeon, T., Paek, I., & Dugarjav, B. (2022). Design and validation of pitch H-infinity controller for a large wind turbine. *Energies*, 15(22), 8763.
- 350 Singh, N., Pratap, B., & Swarup, A. (2016). Design of robust control for wind turbine using quantitative feedback theory. *IFAC-PapersOnLine*, 49(1), 718-723.
- International Electrotechnical Commission. (2020). IEC 61400: Wind energy generation systems.
- Tibaldi, C., Henriksen, L. C., Hansen, M. H., & Bak, C. (2016). Wind turbine fatigue damage evaluation based on a linear model and a spectral method. *Wind Energy*, 19(7), 1289-1306.
- 355 Wöhler, A. (1870). *Über die festigkeitsversuche mit eisen und stahl*. Ernst & Korn.
- Manson, S. S. and Newman, M. E. J. (1994). *Fatigue of Materials*. Springer, New York, 2nd edition edition.
- Wirsching, P. H., & Light, M. C. (1980). Fatigue under wide band random stresses. *Journal of the Structural Division*, 106(7), 1593-1607.
- Benasciutti, D., & Tovo, R. (2005). Spectral methods for lifetime prediction under wide-band stationary random processes. *International Journal of fatigue*, 27(8), 867-877.
- 360 Benasciutti, D. (2012). *Fatigue analysis of random loadings. A frequency-domain approach*. LAP Lambert Academic Publishing AG & Co KG.
- Dirlik, T. (1985). *Application of computers in fatigue analysis* (Doctoral dissertation, University of Warwick).
- OpenFAST. Available at <https://github.com/openfast/openfast/>.
- Abbas, N. J., Zalkind, D. S., Pao, L., & Wright, A. (2022). A reference open-source controller for fixed and floating offshore wind turbines. *Wind Energy Science*, 7(1), 53-73.
- 365 Gaertner, Evan, et al. Definition of the IEA 15-megawatt offshore reference wind turbine. 2020.
- Elso, J., GilMartinez, M., & GarciaSanz, M. (2017). Quantitative feedback control for multivariable model matching and disturbance rejection. *International Journal of Robust and Nonlinear Control*, 27(1), 121-134.
- Yaniv, O., Chait, Y., & Borghesani, C. (1997). The QFT control design toolbox for MATLAB. *IFAC Proceedings Volumes*, 30(16), 103-108.
- 370 Jonkman, B. J. (2006). *TurbSim user's guide* (No. NREL/TP-500-39797). National Renewable Energy Lab.(NREL), Golden, CO (United States).